Part 2: Proper Orthogonal Modal Modeling of a Frictionally Excited Beam

R. V. KAPPAGANTU
Altair Engineering, Inc.
1755 Fairlane Drive
Allen Park, MI 48101 U.S.A.

and

B. F. FEENY
Department of Mechanical Engineering
Michigan State University
East Lansing, MI 48824 U.S.A.

Abstract. Proper orthogonal modes (POMs) are used for order reduction in a beam with frictional excitation. The distributed model is based on an Euler-Bernoulli beam with frictional excitation. The friction is modeled with Coulomb's law and contact compliance, and the contact surface undergoes an imposed oscillation. The POMs are selected from a chaotic response to build the reduced system model. These POMs are extrapolated into proper orthogonal modal functions (POMFs) by using the linear normal modes as basis functions. The POMFs are used as the basis for projection the partial differential equation of motion to a low-order set of ordinary differential equations. Simulated responses based on the POMFs and linear normal modes are compared to that of a "truth set" simulation, which is based on ten linear normal modes.

1 Introduction

In the preceding study [9] we have examined the dynamics of an experimental beam with frictional excitation. This work involved characterization of the dynamical response, and the proper orthogonal decomposition (POD) of displacements on the beam. The discrete proper orthogonal modes (POMs) were extrapolated into continuous proper orthogonal modal functions (POMFs), expressed in terms of the basis functions, which happened to be the theoretical modes of the linear cantilevered beam. A Gramm-Schmidt orthonormalization procedure was employed in this conversion to keep the POMFs orthogonal. The POMFs were compared to the linear normal modes (LNMs) and shown to provide a more efficient basis in terms of signal energy composition. This is sensible since the discrete POMs have been shown to optimize the spatial content of a signal ensemble in terms of signal energy [11, 2].

Earlier studies on POD involved the usage of POMs as empirical modes for reduced order modeling in turbulence [2]. More recent studies have applied the

POMs as empirical modes for the reduced order modeling of structural systems [5, 14, 1, 12]. For symmetric linear vibration systems with known mass distributions, POMs of multi-modal responses converge to the linear normal modes [4, 16]. Furthermore, the dominant POM of a synchronous single-mode nonlinear modal motion represents a best fit of the nonlinear normal mode [4]. Other results [3, 12, 6] support these notions, and suggest that there may be a carry over to multi-modal nonlinear responses.

In this paper, we use the POMFs obtained in the previous experiment as a basis for Galerkin projections of the PDE model of the beam. We compare the POMF projections with LNM projections. We find that in some cases the POMFs are more efficient in the reduced order modeling.

This paper is organized as follows. The next section includes the formulation of the mathematical model for the frictionally excited beam, and outlines the scheme used for simulating the system under the conditions of stick-slip. Section 3 presents numerical simulations of the reduced-order models. Section 4 includes supplementary discussions, and Section 5 concludes the paper.

2 Mathematical Model

The system under consideration [8] consists of a cantilever with an attachment for convenient variation of normal load. Because of the attachment, we have the friction force F acting not on the cantilever, but at the end of an extension. This force can be transferred to the cantilever tip, by an equivalent force and moment combination (the force is F and the moment is Fl, where l is the length of the extension). To take the inertial effects of the extension and the fixture we lump the masses together at the cantilever tip. Hence we need the beam equation where both external forces and moments are present. Assuming that there is no shear, we use the extended Hamilton's principle [13] to get the standard PDE for a Euler-Bernoulli beam and write our system equation as

$$\frac{\partial^2}{\partial x^2}[EI(x)\frac{\partial^2 y(x,t)}{\partial x^2}]+\rho(x)\frac{\partial^2 y(x,t)}{\partial t^2} = p(x,y(x,t),\dot{y}(x,t),t)-\frac{\partial q(x,y(x,t),\dot{y}(x,t),t)}{\partial x} \tag{1}$$

where $y(x,t)$ is the deflection at the point x at time t. $E(x), I(x)$ and $\rho(x)$ are the elastic modulus, the area moment of inertia and the linear density respectively of the system at location x. Linear viscous damping is neglected. Quantities $p(x,y,\dot{y},t)$ and $q(x,y,\dot{y},t)$ are general external forces and moments applied at location x on the beam at time t. Note that p and q are time varying functions of relative velocity, normal load and other parameters in case of frictional excitation. In our case, we accommodate the concentrated force and moment by expressing $p = F\delta(x-L)$ and $q = Fl\delta(x-L)$, where L is the length of the beam. The parameter values were estimated in the experimental study [8].

With this assumption of "an Euler-Bernoulli cantilever beam with a lumped mass at the free end" for the system, we numerically estimated frequencies of 3.13, 21.97, 64.72, 130.64, 220.55 and 334.12 Hz. These frequencies are higher than the experimental frequencies (3.75, 18.4, 53.75, 102.5, 172.5 and 265 Hz), with the exception of the fundamental frequency. Discrepencies may be rooted in the beam-model assumptions, the neglected rotational inertia of the loading-beam attachment, and the quality of the experimental clamp.

As mentioned earlier we use a Galerkin's approximation, based on an orthonormal basis of functions $\{\varphi_1(x), \varphi_2(x), \cdots\}$ which satisfy the boundary conditions, to convert the above PDE (1) into ODEs. As a result, for each $j \in [1,N]$ we have

$$\sum_{i=1}^{N} M_{ji}\ddot{u}_i + \sum_{i=1}^{N} K_{ji}u_i = fP_j, \tag{2}$$

where the u_i are the generalized coordinates associated with the basis functions,

$$\begin{aligned} K_{ji} &= \int_{x=0}^{x=L} EI(x)\varphi_j(x)\varphi_i^{(iv)}(x)dx, && (3)\\ M_{ji} &= \int_{x=0}^{x=L} \rho\varphi_j(x)\varphi_i(x)dx + m_L\varphi_j(L)\varphi_i(L), && (4)\\ P_j &= \varphi_j(L) + l\varphi_j'(L) - l\varphi_j(L), && (5) \end{aligned}$$

and f represents the modulation of the friction force, which depends now on displacement quantities u_i and their time derivatives, and t since the relative velocity is dependent on the reciprocating excitation surface. Assuming $\mathbf{M}$ to be invertible, we can write equation (2) as

$$\ddot{\mathbf{u}} = -\mathbf{M}^{-1}\mathbf{K}\mathbf{u} + \mathbf{M}^{-1}\mathbf{P}f(\mathbf{u}, \dot{\mathbf{u}}, t). \tag{6}$$

Also if we assume that the modal viscous damping is proportional to the stiffness, then the only difference to the above equation would be a term $-c\mathbf{M}^{-1}\mathbf{K}\dot{\mathbf{u}}(t)$ added to the right hand side. Here c would be proportional to a characteristic damping coefficient. Let us now write the system equation with such damping in the state space form, with the elements of the state $\mathbf{U}$ defined by elements $U_1 = u_1, \cdots, U_n = u_n, U_{n+1} = \dot{u}_1, \cdots U_{2n} = \dot{u}_n$. Thus we end up with the following state-space equation:

$$\dot{\mathbf{U}} = \begin{bmatrix} \mathbf{0} & \mathbf{I} \\ -\mathbf{M}^{-1}\mathbf{K} & -c\mathbf{M}^{-1}\mathbf{K} \end{bmatrix} \mathbf{U} + \begin{bmatrix} \mathbf{0} \\ \mathbf{M}^{-1}\mathbf{P} \end{bmatrix} f(\mathbf{U}). \tag{7}$$

For clarity let us denote the coefficient of the state $\mathbf{U}$ as $\mathbf{A}$ and the coefficient of the forcing term $f(\mathbf{U})$ as $\mathbf{B}$. Thus

$$\dot{\mathbf{U}} = \mathbf{A}\mathbf{U} + \mathbf{B}f. \tag{8}$$

These equations can be numerically integrated to find the values of $U_i(t)$, which in turn can be used to obtain the value of $y(x,t)$ and its derivatives at any point on the beam, provided we know f. The quantity f is the same as the frictional forces at the massless contact point, and is implicitly time dependent. When the contact elements are sliding the relative velocity between the contact elements at the point of contact is the same as the relative velocity between the slider and the tip of the beam. Hence in the sliding mode, we have f well defined by the kinetic friction force.

However when the two contact elements are stuck, from the dynamic equilibrium we can verify that the static friction force is in equilibrium with $K_C(Y_T(t) - Y_C(t))$, the elastic force due to contact compliance. Here, Y_C and Y_T are the displacements of the contact surface and the beam tip, and K_C is the contact stiffness. This in turn is the excitation force f. $Y_C(t) = a\sin(\omega t)$, the slider displacement, is imposed. The tip displacement $Y_T(t)$ can be calculated from the state $\mathbf{U}$. Thus we have

$$
\begin{aligned}
f &= K_C(Y_C(t) - Y_T(t)) \\
&= K_C(Y_C(t) - \mathbf{\Psi}^*\mathbf{U}),
\end{aligned} \tag{9}
$$

where

$$
\mathbf{\Psi}^* = [\ \varphi_1(L) + l\varphi_1'(L)\ \ \cdots\ \ \varphi_n(L) + l\varphi_n'(L)\ \ 0\ \cdots\ 0.\ ] \tag{10}
$$

In the above force relation we have the effective force in terms of the state and input displacement which are all known. Thus we know the effective restraining force, which can also be used in comparison with the static friction bounds to determine when the contact elements slip.

3 Numerical Simulations and Validation

We simulate the system based on equations (2)-(5) by using the dominant POMFs identified in the preceding work [9] in the place of the basis functions $\phi_i(x)$. Some of our simulations are based on three ODEs derived by projecting the PDE onto three POMFs from the experiment excited at 12 Hz, while others simulations are based on four ODEs derived by projecting the PDE onto four POMFs obtained from the experiment excited at 41.1 Hz. (The POMs in [9] were obtained from the covariance matrix, meaning that the means of the signals were removed prior to the POD. Technically, these mean values should be incorporated into the Galerkin projection, but as they were small, they are neglected.)

Numerical simulation of stick-slip systems needs to be carried out carefully. The presense of stick and slip leads to an ever changing number of active degrees of freedom, and hence an unsteady topology. General algorithms for handling such systems have been developed [15, 18, 7]. The simulation algorithm needs to keep track of kinematic and kinetic "indicators" of stick and slip and the contact forces, and also incorporate ways of determining the contact forces and reducing the system order as needed. In the particular case of a beam with friction applied at a point, Whiteman and Ferri [17] have outlined an effective method. The algorithm we apply has some similarities, and will be briefly discussed in terms of the formulation in the previous section.

The numerical simulation technique involved the usage of a Runge-Kutta ODE integrator in double precision with a variable-time-step. In our application we have used the full-order set of equations (8) for both stick and slip, and have defined the frictional force based on the kinetic friction coefficient when slipping, and based on equation (9) when stuck. We monitor the sticking friction force in this equation to determine when the static friction is exceeded, such that slip ensues. Using equation (8) for stick means that we are integrating a redundant set of equations. This has not adversely effect the results. It is similar to integrating, for example, the acceleration to obtain the (known) velocity for a stuck belt-driven single-degree-of-freedom friction oscillator.

For a given set of initial conditions we determine the relative velocity and the excitation force. These we use to define a flag for slip or stick. At each time step of integration we determine the relative velocity and effective force on the beam and compare their values for slip and stick criteria. In case of a cross-over (relative velocity crossing zero or the effective force crossing the static friction force bounds) we step back and use a simple interpolation to determine a smaller time step, and integrate again. This we continue until the cross-over is within a predefined tolerance zone. At this point after verifying the respective criterion we move to the subsequent mode. In this way we compute the state $\mathbf{U}$ at each time step which can in turn be used to obtain strain or displacement or velocity at any given point on the beam.

For verification of the friction model that was used in the simulations we illustrate the simulated friction force characteristics in Figure 1. We recorded these measurements using the 3-POMF reduced model (the POMFs derived from the 12 Hz dynamics). These match the characteristics of the compliant contact during stick and stick-slip [10] also obeserved in the experiment [9].

We simulate frequency sweeps in order to compare the model with the experiment [9]. In the experimental system, a close fit of the relationship between the shaker frequency and amplitude is

$$a = 0.0117\left(\frac{\omega}{2\pi}\right)^{-0.9037}. \tag{11}$$

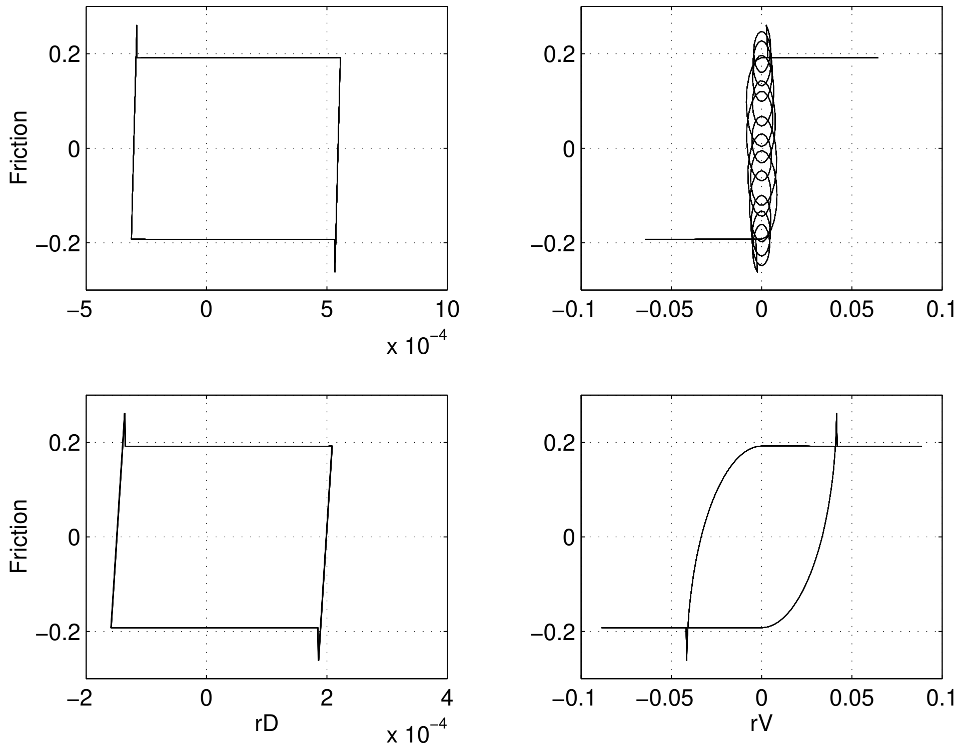

Fig. 1. Simulated friction characteristics of the compliant contact model with $\mu_S > \mu_K$. The top row shows the case of stick-slip and the bottom row shows the case of micro-stick. The left column shows the friction vs. the relative displacement, and the right column depicts the friction vs. the relative velocity.

Here we used the same frequency-amplitude relation in our numerical "frequency" sweeps. Each step in the sweep was carried for 600 cycles of which only the last 100 cycles were stored. Thus we are discarding 500 cycles to account for transients. Incidentally we applied a one-percent proportional damping, and the two-percent settling time is well within this transient time. We however note that the damping effects could be quite different in this nonlinear system. In each of the excitation cycles we computed the strain near the base of the beam, corresponding to the experimental strain gage closest to the clamp, whenever $v(t)$ crosses zero with a positive slope, so as to match the experimental sweeps [9]. Thus we simulated 100

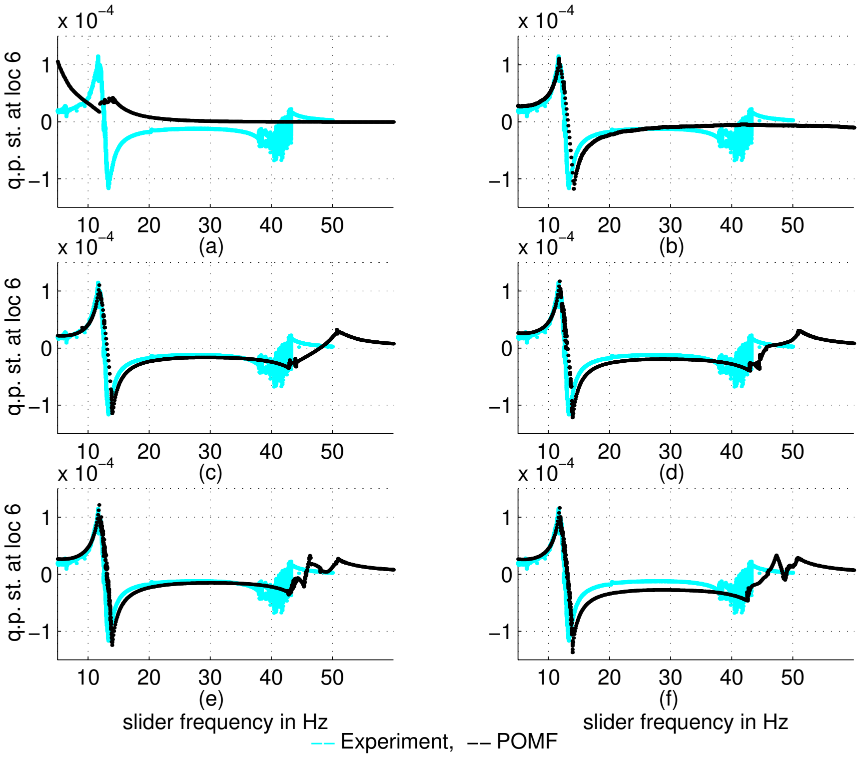

Fig. 2. "Frequency sweeps" of reduced models obtained at different levels of reduction (a-1,b-2,c-3,d-4,e-5,f-6) using POMFs (extracted from experiment at 12.0 Hz and the continuous versions orthonormalized) superimposed on the experimental sweep. The grey curve is experimental, and the solid black curve is simulated.

strain values at each frequency step when the slider acceleration crossed its peak. We swept from $5-60$ Hz in steps of 0.1 Hz. We caution the reader that the above plots are not the amplitude-frequency response curves. These plots can be viewed as sweeps of Poincaré sections, projected onto a single coordinate axis, along the parameter-space curve described by the equation (11).

In Figure 2 we show the sweeps obtained from based on POMFs determined at 12.0 Hz in the physical experiment superimposed on the experimental frequency sweep.

From these plots we see that the most dominant mode alone is not able to predict the system's behavior. With two dominant modes we are able to retrieve the resonant dynamics around 12 Hz range (the POMs are extracted from the chaotic orbits at this frequency), but the high frequency dynamics are not realized. However with three POMs we are able to see the higher resonant frequencies, though the higher periodic and nonperiodic responses (indicated by the smear of points) are not as pronounced as in the experiment. These nonperiodicities become more prominent as we include more POMs but the sweep characteristics (represented by the resonant frequencies) remain same. The inclusion of higher modes results in higher computing time, which grows exponentially with increasing number of modes.

On comparing these predicted sweeps with the ones from the experiment we realize that though the stick-slip higher periodic or nonperiodic responses around 12 and 41 Hz of the physical experiment do occur, the latter nonperiodicities occur at slightly higher frequencies. The nonperiodic dynamics in the predicted sweeps is not as prominent as in the experiment, especially at the higher frequencies. However we note that the periodic orbits and also the zones of pure stick, which occupy broad regions between the resonances, are well predicted by the reduced model.

In order bypass the uncertainities involved in our modeling efforts, viz., beam model, damping, friction characteristics, etc., we considered a model similar to that of the POMF model, but with a large number of LNMs (ten) as a "truth set". We compared the frequency sweeps of reduced models with that of this "truth set" (see Figure 3). This comparison reveals that the resonant frequencies predicted by the POMF models are almost same as the ones predicted by the "truth set" model. The convergence of the reduced model frequency sweep with that of the "truth set" is acheived rather earlier just with three POMFs.

In this particular system we were fortunate to have the LNMs of the linear cantilever readily available. As such we built reduced models with the LNMs and carried frequency sweeps similar to those of POMF models, and present these in Figure 4. From Figures 3 and 4 we realize that in this particular example POMFs have faster convergence than the LNMs.

In Figure 5 we show the sweeps obtained from the POMFs determined at 41.1

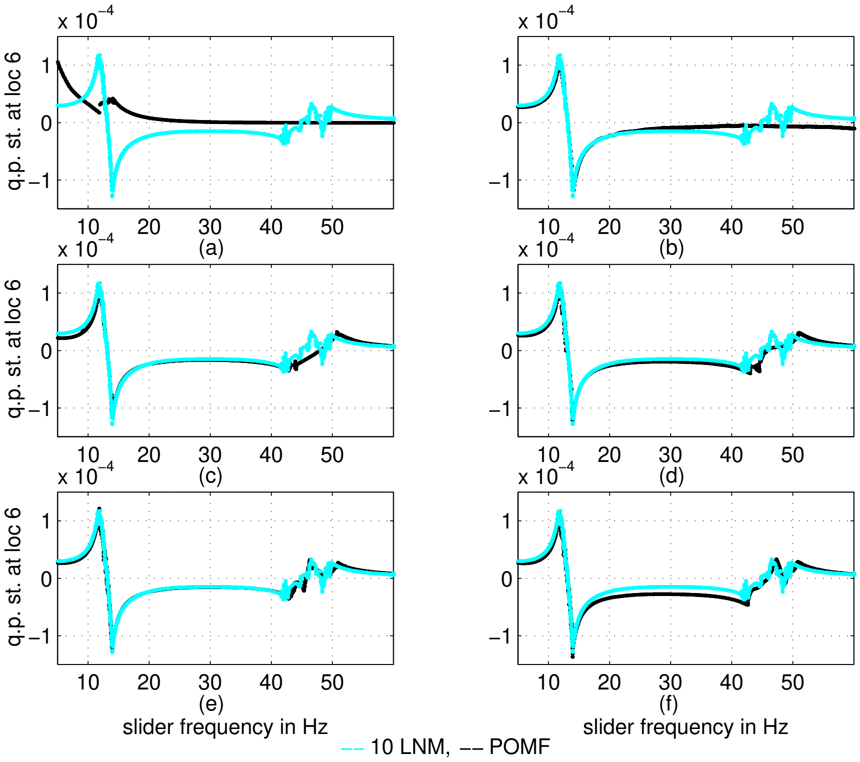

Fig. 3. "Frequency sweeps" (black) of reduced models obtained at different levels of reduction (a-1,b-2,c-3,d-4,e-5,f-6) using POMFs (extracted from experiment at 12.0 Hz and the continuous versions orthonormalized) superimposed on frequency sweep (grey) obtained from 10-LNM model ("truth set").

Hz in the physical experiment superimposed on the experimental sweep.

We recall that four of this set of POMFs were dominant (whose combined energy content is at least 99.99%). The above plots indicate that many of the rough features of the dynamics are revealed when at least four POMFs are used in the model. The models built by using less than four POMFs from the 41.1 Hz dynamics did not reveal the higher resonant frequencies. Also the dynamics in the 12 Hz neighborhood predicted by these models deviated from that of the experimental sweeps. However with four POMFs model the deviation is reduced and also the higher resonant dynamics are revealed.

For the three POMF reduced model (from the 12.0 Hz chaotic dynamics in

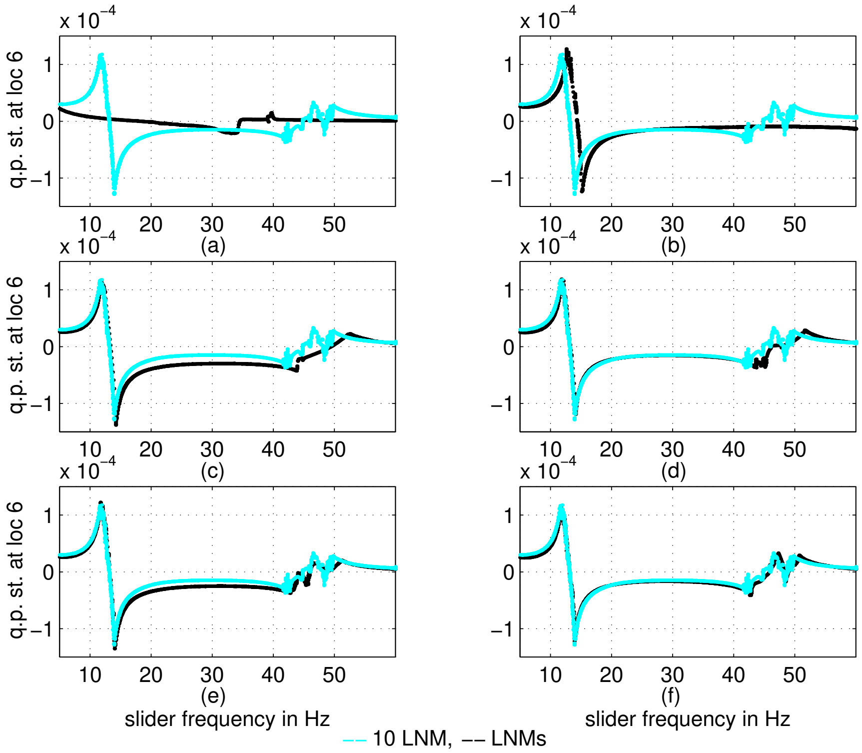

Fig. 4. "Frequency sweeps" (black) of reduced models obtained at different levels of reduction (a-1,b-2,c-3,d-4,e-5,f-6) using LNMs of the cantilever superimposed on frequency sweep (grey) obtained from 10-LNM model ("truth set").

the experiment) we show the phase portraits (displacement versus velocity of the contact point on the beam) in Figure 6. These are obtained at 11, 11.9 and 42.9 Hz respectively of the resulting dynamics in the sweeps. These may be compared with the experimental phase-portraits [9].

4 Discussion

We have taken a set of proper orthogonal modes from the response at a single parameter set and used them as the foundation for reduced order modeling of the beam equations. The resulting low-order model was then simulated for a parameter range (frequency sweep) and compared to the experiment. There is no reason to

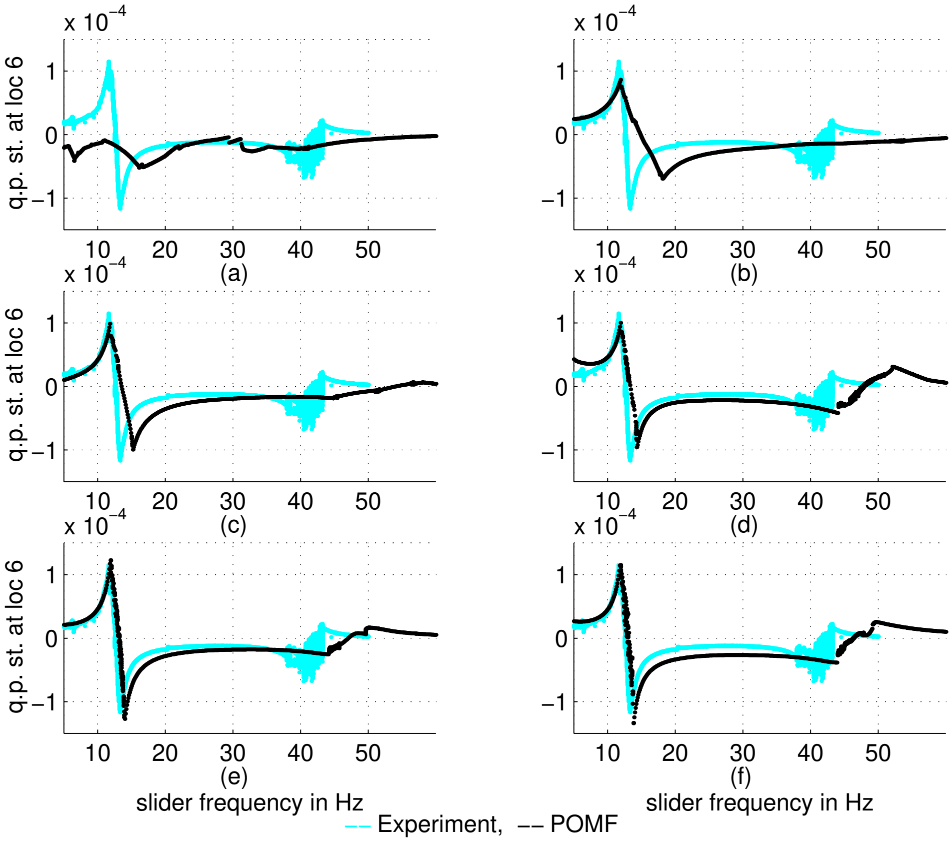

Fig. 5. "Frequency sweeps" of reduced models obtained at different levels of reduction (a-1,b-2,c-3,d-4,e-5,f-6) using POMFs (extracted from experiment at 41.1 Hz and the continuous versions orthonormalized) superimposed on the experimental sweep. The grey curve is experimental, and the solid black curve is simulated.

assume that the POMs found at 12 Hz (or 41.1 Hz) should represent the dynamics at any other frequency, or at other choices of initial conditions. However, in this case the extrapolation of the POM-based model to other parameter values has drawn out some of the dynamical features.

In our projections, we started with POMs obtained from discrete measurements, and used them to fit continous POMFs. While the POMs represent optimal energy distributions of the data, there is no such guarantee for the POMFs. We had seen, however, that as large numbers of redundant false sensors were added (in the

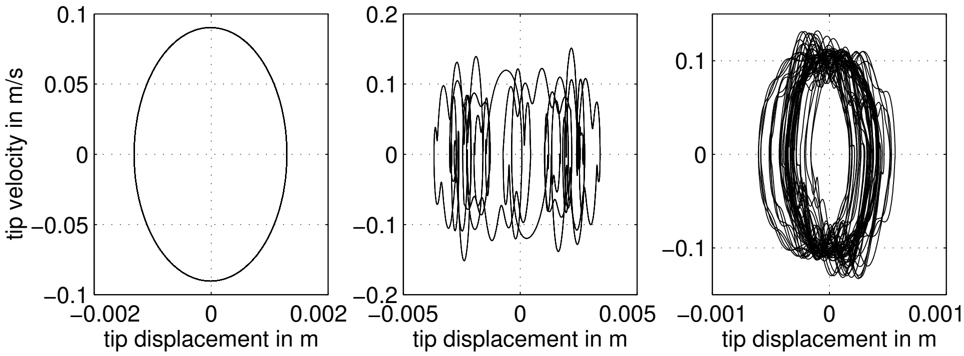

Fig. 6. Phase-portraits (contact point displacement versus velocity) from the three-POMF reduced model at 11, 11.9 and 42.9 Hz.

conversion from strain to displacement, a set of basis functions were used, and these could be evaluated at any number of positions) [9, 8], the discrete POMs seemed to converge closely to the POMFs, indicating that the POMFs are close to optimal. In the reduced order modeling, continuous POMFs were integrated into the PDE to obtain the ODEs. We could have used discrete POMs, and applied them to the PDE by means of a numerical quadrature to obtain ODEs. Indeed, in some applications were the PDE is not so simply defined, this may be a more sensible approach.

We have also performed simulations which incorporated rigid contacts as opposed to compliant contacts [8]. The results with the rigid contacts did not agree as well with experiments as the simulations with compliant contacts. The rigid contacts were unable to generate resonances in the 40 Hz area. Previous work has shown that the dynamic hysteretic effects of compliant contacts are more significant as the frequency increases [10]. It might be interesting to investigate high-frequency applications such as squeak and squeal to find out whether contact compliance is significant to these phenomena, and whether it has a stabilizing or destabilizing effect.

5 Conclusions

In this paper we reduced the order of a nonlinear beam model by using proper orthogonal decomposition, and evaluated the model using frequency sweeps. Though we found some discrepancies between the physical and numerical experiments, we attribute these discrepancies to the original mathematical model of the system, such as the assumptions of Euler-Bernoulli model for the cantilever, lumped mass for the loading beam and friction law to be a simple Coulomb with contact compliance characteristic.

We used POMs obtained from the chaotic dynamics at 12.0 Hz, three of which captured 99.99 % of the signal power, and fit POMFs to these POMs using linear normal modes as basis functions. We then reduced the PDE model by using the POMFs, and compared simulations to experimental results, and to simulations based on LNMs. From the comparison between the LNMs and POMFs we realized that the POMF models converge to both the experimental sweep and the sweep from the "truth set", rather fast with just three POMFs. This is consistent with observations of others [1]. Also the experimental nature of the determination of POMFs makes it more advantageous as for complex systems the LNMs may not be readily available.

We saw in the preceding work that at 41 Hz, the data required more POMs to account for the same signal energy as in the 12 Hz data. Indeed, simulations based on the 41 Hz modes required more modes to pick out the resonance features in the response. We also saw that the POMs were more efficient in capturing the signal energy than the LNMs. Likewise, simulations with POMFs were slightly more effective in order reduction than simulations with the same number of LNMs.

Finally, we have seen that frictional contact compliance may have significant effects on the dynamic response, especially at higher frequencies.

6 Acknowledgements

Support for this research program comes gratefully from the National Science Foundation (CMS-9624347). We appreciate comments from Alan Haddow, Charles

MacCluer, Clark Radcliffe and Steve Shaw.

References

1. M. F. A. Azeez and A. F. Vakakis. Using Karhunen-Loève decomposition to analyze the vibroimpact response of a rotor. In *Proceedings in Seventh Conference on Nonlinear Vibrations, Stability and Dynamics of Structures*, Blacksburg, July 1998.
2. G. Berkooz, P. Holmes, and J. L. Lumley. The proper orthogonal decomposition in the analysis of turbulent flows. In *Annual Review of Fluid Mechanics*, volume 25, pages 539–575. Annual Reviews Inc., 1993.
3. M. A. Davies and F. C. Moon. Solitons, chaos, and modal interactions in periodic structures. In *Nonlinear Dynamics: the Richard Rand 50th Anniversary Volume*, pages 119–143. World Scientific, Singapore, 1997.
4. B. Feeny and R. Kappagantu. On the physical interpretation of proper orthogonal modes in vibrations. *Journal of Sound and Vibration*, 211(4):607–616, 1998.
5. Philip M. Fitzsimons and Chunlei Rui. Determining low dimensional models of distributed systems. *Advances in Robust and Nonlinear Control Systems, ASME DSC*, 53:9–15, 1993.
6. I. T. Georgiou, I. Schwartz, E. Emaci, and A. Vakakis. Interaction between slow and fast oscillations in and infinite degree-of-freedom linear system coupled to a nonlinear subsystem: Theory and experiment. *Journal of Applied Mechanics*, 66(2):448–459, 1999.
7. Ch. Glocker and F. Pfeiffer. Dynamical systems with unilateral constraints. *Nonlinear Dynamics*, 9(3):245–259, 1992.
8. R. V. Kappagantu. *An "Optimal" Modal Reduction of Systems with Frictional Excitation.* Ph.D. thesis, Michigan State University, East Lansing, 1997.
9. R. V. Kappagantu and B. F. Feeny. *Part 1: Dynamical Characterization of a Frictionally Excited Beam.* submitted to Nonlinear Dynamics, 2000.
10. J.-W. Liang and B. F. Feeny. Dynamical friction behavior in a forced oscillator with a compliant contact. *Journal of Applied Mechanics*, 65(1):250–257, 1998.
11. J. L. Lumley. The structure of inhomogeneous turbulent flow. In *Atmospheric Turbulence and Radio Wave Propagation*, pages 166–178. Nauka, Moscow, 1967.
12. X. Ma, M. A. F. Azeez, and A. F. Vakakis. Nonparametric nonlinear system identification of a nonlinear flexible system using proper orthogonal mode decomposition. In *Proceedings in Seventh Conference on Nonlinear Vibrations, Stability and Dynamics of Structures*, Blacksburg, July 1998.
13. Leonard Meirovitch. *Analytical Methods in Vibrations.* Macmillan, New York, 1967.
14. K. D. Murphy. Using the Karhunen-Loève decomposition to examine chaotic snap-through oscillations of a buckled plate. In *Proceedings in Sixth Conference on Nonlinear Vibrations, Stability and Dynamics of Structures*, Blacksburg, June 1996.
15. F. Pfeiffer and Ch. Glocker. *Multibody dynamics with unilateral contacts.* Wiley, New York, 1996.
16. M. S. Riaz and B. F. Feeny. Proper orthogonal decomposition of an experimental cantilever beam. In *Proceedings of the 1999 ASME Design Engineering Technical Conferences*, pages CD–ROM, Las Vegas, September 1999.
17. W. E. Whiteman and A. A. Ferri. Multi-mode analysis of beam-like structures subjected to displacement-dependent dry-friction damping. *Journal of Sound and Vibration*, 207(3):403–418, 1997.
18. M. Wosle and F. Pfeiffer. Dynamics of multibody systems containing dependent unilateral constraints with friction. *Journal of Vibration and Control*, 2(2):161–192, 1996.